

# Tunable Two-Dimensional Non-Close-Packed Microwell Arrays Using Colloidal Crystals as Templates

Zhiyu Ren,<sup>†,‡</sup> Xiao Li,<sup>†</sup> Junhu Zhang,<sup>†</sup> Wei Li,<sup>†</sup> Xuemin Zhang,<sup>†</sup> and Bai Yang<sup>\*,†</sup>

Key Laboratory for Supramolecular Structure and Materials, College of Chemistry, Jilin University, Changchun 130012, and Laboratory of Physical Chemistry, School of Chemistry and Materials Science, Heilongjiang University, Harbin 150080, People's Republic of China

Received February 6, 2007. In Final Form: May 11, 2007

In this paper we demonstrate a facile and efficient way to fabricate poly(dimethylsiloxane) (PDMS) molds with hexagonal non-close-packed (ncp) arrangements of microwells by casting PDMS prepolymer onto two-dimensional (2D) ncp colloidal crystals. The templates of the 2D ncp colloidal crystals were fabricated via coupling lift-up soft lithography and solvent-swelling. We found that the depths of the microwells together with the lattice spacing can be adjusted by the sphere interstices and chemical composition of the 2D ncp colloidal crystals. The relationship of the surface character of the templates with the depths of the microwells can be explained by the wetting behavior of PDMS prepolymer on the rough surface. Contact angle measurements are consistent with the experimental results of the microwells in depth and agree well with the Cassie–Baxter theory. There are at least three advantages of the approach. First, the depth and distance of the microwells can be controlled. Second, PDMS molds can be easily peeled from the surfaces of the templates, which results in reusing the original templates to make new molds. Third, this method can be applied to other materials, such as photopolymerizable resin or thermosetting resin. The potential application of the microwells is as microlenses to make a pattern or as microvials in bioanalytical techniques.

## Introduction

Two-dimensional (2D) porous substrates have attracted great attention for a wide range of applications including chemical microcontainers, surface-plasmon resonance biosensors, catalytic supports, and photonic crystals. Besides traditional lithography methods, which suffered from the disadvantage of high cost, several self-assembly techniques employing block copolymers<sup>1</sup> and colloidal spheres have been used to create microporous materials. Specifically, well-organized 2D particle arrays are of practical significance for applications as they provide simple and cost-effective lithography masks to create regular patterned arrays.<sup>2–10</sup> For example, monolayer or double-layer colloidal crystals have been used as either etching or deposition masks to define mosaic arrays of microcolumnar structures within the interstices of the spheres or to form wells with reasonably good local order on the substrates.<sup>11–14</sup> This strategy is well developed

as colloidal lithography (CL). Besides their applications as masks, self-assembled spheres can also be used as nanosphere molds. Hemispherical wells in silicon and inverse wells have been generated by laser-assisted embossing and replica molding through poly(dimethylsiloxane) (PDMS) soft lithography.<sup>5,15,16</sup>

As self-assembled 2D colloidal crystals in CL are densely packed in the substrates, the resultant pores are interconnected, which is undesired in many applications such as subwavelength optics,<sup>2</sup> single-quantum-dot spectroscopy,<sup>7</sup> surface plasmonic devices,<sup>17</sup> and making a tunable superhydrophobic pattern.<sup>18,19</sup> Multiple steps are required to make isolated nanowell arrays in these fields. If 2D non-close-packed (ncp) colloidal crystals are used in CL, it will be easy to obtain ncp nanowell arrays. Some processes such as template-induced assembly,<sup>20</sup> controlled reactive ion etching,<sup>9</sup> and manipulation of dipole–dipole interaction<sup>21</sup> have been developed, but these approaches involve either expensive lithographic patterning or limitation to achieve acceptable throughputs. Jiang et al.<sup>10</sup> have developed a simple spin-coating technique to make 2D large-scale ncp colloidal crystal–polymer nanocomposites rapidly, but the distance between the centers of adjacent wells is limited at around  $1.4D$ , where  $D$  is the diameter of the as-applied spheres. A grand challenge for the field remains how to adjust the interstices of the colloidal crystals accurately.

Recently, we reported the utilization of the solvent-swelling and mechanical deformation behaviors of PDMS to adjust the

\* To whom correspondence should be addressed. E-mail: byangchem@jlu.edu.cn. Phone: 86-0431-85168478. Fax: 86-0431-85193423.

<sup>†</sup> Jilin University.

<sup>‡</sup> Heilongjiang University.

(1) Jenekhe, S. A.; Chen, X. L. *Science* **1999**, *283*, 372–375.

(2) Abdelsalam, M. E.; Bartlett, P. N.; Baumberg, J. J.; Coyle, S. *Adv. Mater.* **2004**, *16*, 90–93.

(3) Sun, F. Q.; Cai, W. P.; Li, Y.; Cao, B. Q.; Lei, Y.; Zhang, L. D. *Adv. Funct. Mater.* **2004**, *14*, 283–288.

(4) Cho, Y. H.; Cho, G.; Lee, J. S. *Adv. Mater.* **2004**, *16*, 1814–1817.

(5) Barton, J. E.; Odom, T. W. *Nano Lett.* **2004**, *4*, 1525–1528.

(6) Lu, Y.; Xiong, H.; Jiang, X.; Xia, Y. N.; Prentiss, M.; Whitesides, G. M. *J. Am. Chem. Soc.* **2003**, *125*, 12724–12725.

(7) Hakanson, U.; Persson, J.; Persson, F.; Svensson, H.; Montelius, L.; Johansson, M. K. J. *Nanotechnology* **2003**, *14*, 675–679.

(8) McLellan, J. M.; Geissler, M.; Xia, Y. N. *J. Am. Chem. Soc.* **2004**, *126*, 10830–10831.

(9) Choi, D. G.; Yu, H. K.; Jang, S. G.; Yang, S. M. *J. Am. Chem. Soc.* **2004**, *126*, 7019–7025.

(10) Jiang, P. *Angew. Chem., Int. Ed.* **2004**, *43*, 5625–5628.

(11) Deckman, H. W.; Dunsmuir, J. H. *Appl. Phys. Lett.* **1982**, *41*, 377–379.

(12) Haynes, C. L.; Van Duyne, R. P. *J. Phys. Chem. B* **2001**, *105*, 5599–5611.

(13) Wang, X. D.; Graugnard, E.; King, J. S.; Wang, Z. L.; Summers, C. J. *Nano Lett.* **2004**, *4*, 2223–2226.

(14) Kei, C. C.; Kuo, K. H.; Su, C. Y.; Lee, C. T.; Hsiao, C. N.; Perng, T. P. *Chem. Mater.* **2006**, *18*, 4544–4546.

(15) Wu, M. H.; Park, C.; Whitesides, G. M. *J. Colloid Interface Sci.* **2003**, *265*, 304–309.

(16) Nam, H. J.; Jung, D. Y.; Yi, G. R.; Choi, H. *Langmuir* **2006**, *22*, 7358–7363.

(17) Jiang, P.; McFarland, M. J. *J. Am. Chem. Soc.* **2005**, *127*, 3710–3711.

(18) Han, J. T.; Lee, D. H.; Ryu, C. Y.; Cho, K. *J. Am. Chem. Soc.* **2004**, *126*, 4796–4797.

(19) Yan, L. L.; Wang, K.; Wu, J. S.; Ye, L. *J. Phys. Chem. B* **2006**, *110*, 11241–11246.

(20) Yin, Y. D.; Lu, Y.; Gates, B.; Xia, Y. N. *J. Am. Chem. Soc.* **2001**, *123*, 8718–8729.

(21) Lumsdon, S. O.; Kaler, E. W.; Williams, J. P.; Velev, O. D. *Appl. Phys. Lett.* **2003**, *82*, 949–951.

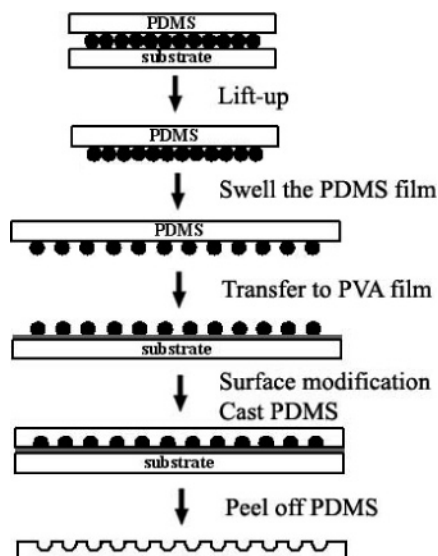


**Figure 1.** A schematic illustration of the procedure for the fabrication of 2D ncp microwell arrays by using silica spheres as the template.

lattice structures of 2D sphere arrays. More importantly, the as-prepared 2D ncp sphere arrays could be kept and transferred onto the surface of a solid substrate by using a modified microcontact printing ( $\mu$ cp) technique.<sup>22</sup> In this paper, we present the utilization of 2D ncp colloidal crystals to mold PDMS with hemispherical microwell arrays on the surface. Furthermore, the lattice spacing and depth of the microwells can be adjusted by changing the interstices and surface character of the colloidal spheres. The main practical purpose of this work is to develop a facile and effective strategy leading to fabrication of ncp microwells.

### Experimental Section

**Materials.** Silicon substrates were cleaned by immersion in piranha solution (3:1 concentrated  $\text{H}_2\text{SO}_4$ /30%  $\text{H}_2\text{O}_2$ ) for 1 h at 70 °C to create a hydrophilic surface and then rinsed repeatedly with Milli-Q water (18.2  $\text{M}\Omega\text{ cm}^{-1}$ ) and ethanol. The substrates were dried in nitrogen gas before used. The silica microspheres were prepared by the Stöber method,<sup>23</sup> and their average sizes were measured as 1.115  $\mu\text{m}$  by SEM with a calibrated length. Octyltrichlorosilane (OTS) and PDMS elastomer kits (Sylgard 184) were purchased from Aldrich and Dow Corning (Midland, MI), respectively. Sulfuric acid, hydrogen peroxide, poly(vinyl alcohol) (PVA), dichloromethane ( $\text{CH}_2\text{Cl}_2$ ), and dimethyldichlorosilane ( $(\text{CH}_3)_2\text{Cl}_2\text{Si}$ ) were used as received.

**Preparation.** Figure 1 outlines the procedure for the fabrication of 2D ncp microwell arrays with tunable lattice structures. 2D ncp colloidal monolayers of 1.115  $\mu\text{m}$  silicon spheres were prepared as reported earlier.<sup>22</sup> The molds were prepared by casting PDMS prepolymer onto the microsphere-covered substrates. After being treated under vacuum (0.09 MPa) for 1 h to remove the entrained gas and cured in a conventional drying oven at 60 °C for 3 h, the PDMS molds were peeled from the silica templates. To change the chemical composition of the surface, the templates were treated by plasma etching and silane. The plasma etching was performed using PVA Tepla O-Plasma System 100 with  $\text{O}_2$  (100 mL/min) at a power density of 150 W for 30 s. After the plasma treatment, all templates were subjected to an annealing treatment in an oven at 100 °C for 1 h to moderate the surface roughness of the templates caused by plasma processing. The templates were chemically modified by  $(\text{CH}_3)_2\text{Cl}_2\text{Si}$  and OTS molecules. The microsphere-covered substrates were immersed into a 0.25 wt % solution of  $(\text{CH}_3)_2\text{Cl}_2\text{Si}$  (or OTS)

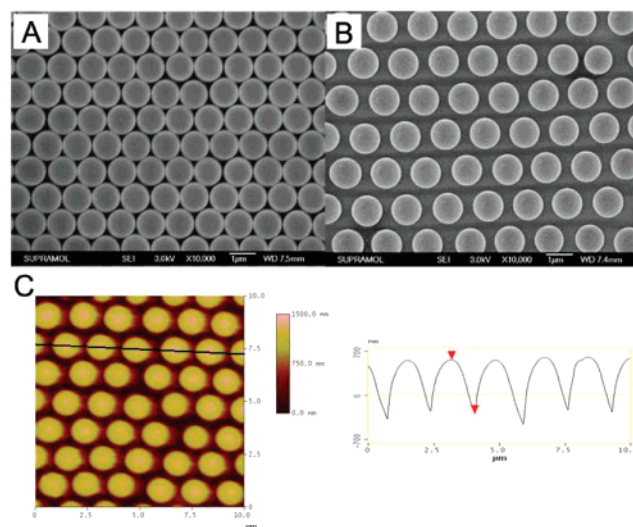


**Figure 2.** (A) SEM image of 2D hexagonal close-packed silica spheres on the silicon wafer. (B) SEM image of 2D ncp silica spheres on the PVA-covered substrate. (C) AFM image and line profile of 2D hexagonal ncp silica spheres on the PVA-covered substrate.

in  $\text{CH}_2\text{Cl}_2$  at room temperature for 1 h to deposit the silane onto the surfaces, then rinsed with  $\text{CH}_2\text{Cl}_2$ , and dried with nitrogen gas.

**Characterization.** AFM images were recorded in the contact mode with a Nanoscope IIIa scanning probe microscope from Digital Instruments under ambient conditions. SEM micrographs were taken with a JEOL JSM 6700F field emission scanning electron microscope with a primary electron energy of 3 kV, and the samples were sputtered with a layer of Pt (ca. 2 nm thick) prior to imaging to improve conductivity. Contact angle measurements were made using PDMS prepolymer and water after surface treatment immediately. All of the measurements were performed at room temperature using a drop shape analysis system (DSA 10 MK2, KRÜSS). At least 10 measurements were averaged for all of the data reported here.

### Results and Discussion

**2D ncp Arrays of Colloidal Spheres.** Many methods have emerged for self-assembly of close-packed colloidal crystals in the past decade. We apply the procedure developed by Micheletto<sup>24</sup> for colloidal array fabrication here because of its simplicity. Figure 2A shows a typical SEM image of the ordered array of silica spheres. Every silica sphere with an average diameter ( $D$ ) of 1.115  $\mu\text{m}$  arrayed in the classic hexagonal lattice structure. Usually, intrinsic point and line defects appear in the resulting structure, and typical defect-free domain sizes are in the 10–50  $\mu\text{m}^2$  range. By using lift-up soft lithography and solvent-swelling, 2D hexagonal ncp sphere arrays on PVA-coated substrate are shown in Figure 2B. The lattice spacing of the obtained crystal structure is extended to about 1.40 $D$ , while the highly ordered hexagonal arrangement is preserved. The ncp structures of the sphere arrays are mechanically stable because the spheres sank into the PVA film during the  $\mu$ cp process. The average height of the exposed silica sphere is about 879 nm, less than the diameter, as shown in Figure 2C. For the typical sample, we could modulate the lattice spacing from 1.00 $D$  to 1.47 $D$  by changing the swollen ratio; furthermore, by combining mechanical stretching, we could adjust the lattice spacing to a larger size.

**PDMS Molds with 2D Hexagonal ncp Microwell Arrays.** We pour PDMS prepolymer onto the microsphere-covered substrates to obtain the PDMS molds, which give patterned hemispherical microwells in the hexagonal ncp lattice after curing,

(22) Yan, X.; Yao, J. M.; Lu, G.; Li, X.; Zhang, J. H.; Han, K.; Yang, B. J. *Am. Chem. Soc.* **2005**, 127, 7688–7689.

(23) Stöber, W.; Fink, A.; Bohn, E. J. *Colloid Interface Sci.* **1968**, 26, 62–69.

(24) Micheletto, R.; Fukuda, H.; Ohtsu, M. *Langmuir* **1995**, 11, 3333–3336.



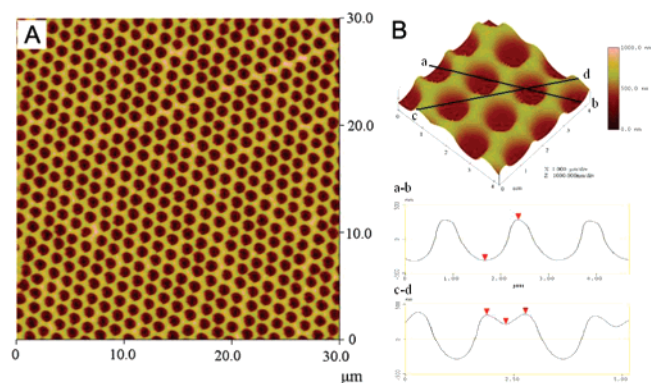
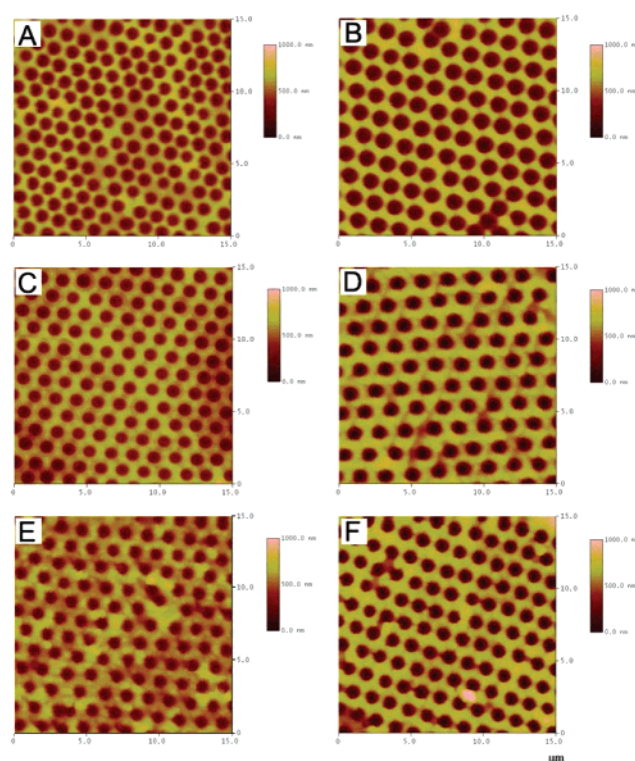


**Figure 3.** (A) AFM images of 2D hexagonal ncp microwells on the PDMS mold fabricated by using silica spheres as the template. The sphere interstices are  $0.40D$ . (B) Typical 3D image and the line profiles.

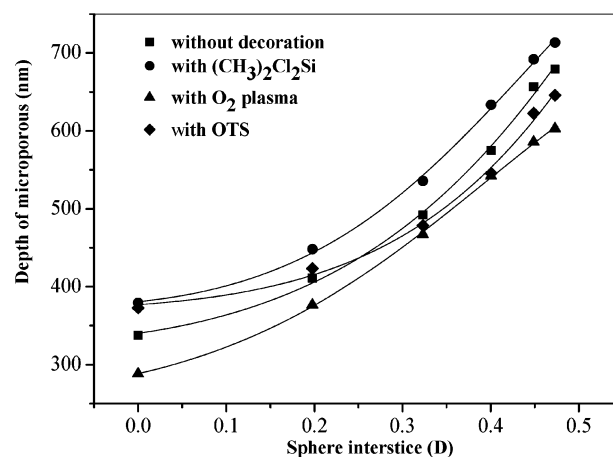
as shown in Figure 3. Two competitive factors should be considered during choosing the ratio of the silicon elastomer and the curing agent: (i) the prepolymer gives less viscous characteristics to improve the effective penetration into the voids of silica sphere arrays by capillary action during replica molding, which needs a high curing agent ratio; (ii) the prepolymer has enough time to penetrate into the voids, which needs a low curing agent ratio. Here we choose a 10:0.7 mixture of silicon elastomer and the curing agent to make the PDMS prepolymer infiltrate the interstices as much as possible and easy to peel from the templates.

Figure 3 displays the topography of the PDMS mold replicated from the template with  $0.40D$  sphere interstices. The line profile of the a–b direction shows that the average feature size of microwells in width is appreciably bigger than the diameter of the spheres ascribed to the viscous behavior of PDMS prepolymer, which makes the PDMS prepolymer partly contact the surfaces of the silica templates during infiltration and results in formation of open microwells. The average depth of the microwells (575 nm), which is only half the diameter of the spheres, implies that the prepolymer cannot penetrate into the interstices absolutely. This is due not only to the small interstices between two neighboring spheres along the edge direction for prepolymer to infiltrate, but also to the difficult to remove residual gas in it, which results in pressure to restrain the penetration of the prepolymer. In the case of a bigger void volume of triangle interstices, however, the protrusions with pyramid-shaped geometry on the PDMS molds can penetrate more compared to the interstices in the a–b direction, so the protrusions aligned along the c–d direction exhibit interesting saddle-sharp structures, which originate from the discrepancy of the infiltration degree between the interstices of two neighboring spheres and the voids among three spheres. The average size of the saddle-sharp structure is 878 nm in width and 128 nm in depth. Other PDMS molds, prepared by modulating the sphere interstices of the templates via solvent-swelling, have a similar geometry with different feature sizes.

**Effects of the Surface Characteristics on the Depths of the Microwells.** In our previous study, the lattice spacing of the microsphere arrays could be flexibly controlled by adjusting the swelling magnitude of the PDMS film.<sup>22</sup> Using the microsphere arrays as templates, the interstices of neighbor microwells can also be controlled. Parts A and B of Figure 4 show the morphologies of PDMS molds with different sphere interstices, and the change tendency in the interstices of the microwells is similar to that of the lattice spacing of the spheres. Moreover, AFM images display the average feature sizes of the microwells



**Figure 4.** AFM image of 2D hexagonal ncp microwells on the PDMS molds fabricated by silica spheres. (A), (C), and (E) show the sphere interstices are  $0.20D$ , and (B), (D), and (F) show the sphere interstices are  $0.47D$ . (A, B) Molding from the original sphere. (C, D) The silica spheres were silanized by immersion in  $(\text{CH}_3)_2\text{Cl}_2\text{Si}$ . (E, F) The silica spheres were subjected to plasma etching, followed by an annealing treatment before casting of PDMS prepolymer.



**Figure 5.** Dependence of the depths of the microwells on the sphere interstices of the templates.

in depth increase with augmenting the sphere interstices of the templates, from 335 to 677 nm, as shown in Figure 5 (squares).

The process of fabricating microwells can be explained using the wetting behavior of PDMS prepolymer on the rough surface. Wettability is one of the important properties of solid surfaces governed by both the surface topography and the chemical composition of the solid surfaces. Although it has attracted great interest for both fundamental research and practical applications,<sup>18,19,25,26</sup> nearly all of the significant results are based on the actions of water. The current system involved a reverse state because PDMS prepolymer, instead of water, is a low-surface-energy material.

**Table 1. Surface Character Effects of 2D ncp Microspheres on PDMS Prepolymer Contact Angles (deg)**

sphere interstice ( $\times D$ )	contact angle (deg)			
	original	plasma	(CH <sub>3</sub> ) <sub>2</sub> Cl <sub>2</sub> Si	OTS
0.00	123.6	125.3	121.2	122.4
0.20	121.9	122.9	119.1	121.0
0.32	117.3	120.6	116.3	119.4
0.40	116.5	119.9	115.7	120.2
0.45	115.5	119.6	114.5	118.1
0.47	116.9	120.7	115.3	119.1

It is reported that the hydrophobicity of a surface can be adjusted by surface roughness within a special size. Two distinct wetting behaviors, namely, Wenzel theory and Cassie–Baxter theory, have been observed depending upon the nature and extent of the surface roughness. In the two regimes, the hydrophobicity of a rough surface is augmented by the increase and decrease of the solid–liquid contact area, respectively.<sup>27</sup> Moreover, when the roughness factor exceeds a certain level ( $\sim 1.7$ ), the contact angle continues to increase, while the dominant hydrophobicity mode switches from Wenzel to Cassie–Baxter due to the increase of the air fraction at the interface between the solid and water.<sup>28</sup> Furthermore, it is noteworthy that the Wenzel roughness factor of the hexagonal close-packed (hcp) particulate monolayer is 1.9.<sup>29</sup> The Cassie–Baxter theory, therefore, is applicable to the current system. It implies that wetting of PDMS prepolymer on the ncp silica spheres improves by increasing the interstices of the spheres. To elaborate this argument, PDMS prepolymer contact angles on the original silica spheres are listed in Table 1. The contact angles decrease with increasing interstices of the silica spheres, which is consistent with the prediction. Furthermore, it is noteworthy that the change of contact angles also decreases and the contact angle especially disagrees with Cassie–Baxter’s mode, when the interstices of the spheres reach  $0.47D$ . This contradiction may be due to the transition of the contact mode. PDMS prepolymer droplets probably are on the interstices of the spheres with increasing lattice spacing of the microsphere arrays. In this case, the PDMS droplets tend to wet the whole area underneath; that is, the Wenzel mode is dominant instead of the Cassie–Baxter mode. To verify the conclusion, we also measure the water contact angles on templates with different interstices of the spheres. The reverse change is shown in Table S1 in the Supporting Information, as we mentioned above.

On the other hand, the effect of the gravitation of PDMS droplets in the system is another noticeable factor. It is obvious that the bigger the interstices of the spheres, the easier the PDMS prepolymer penetrates into the voids, which consequentially results in the sizes of the microwells still increasing in depth, although the wettability of PDMS prepolymer on the colloidal spheres decreases. All factors probably work in combination and contribute to the consequence that the depth of the microwells is an exponential function of the sphere interstices, as shown in Figure 5.

Besides the surface roughness of the templates, the chemical composition can also change the wetting behavior of PDMS prepolymer on the ncp silica spheres. In the study reported herein, we modify the surface of the sphere-covered substrates by silane

and using plasma etching. The highly ordered hexagonal arrangement is also preserved, and the surface roughness is induced on the PDMS molds, as shown in Figure 4. Furthermore, the change of the depths and contact angles of the microwells is presented in Figure 5 and Table 1, respectively.

First, we introduce hydrophobic silane ( $-\text{Si}(\text{CH}_3)_2-$ ) groups on the silica spheres by dipping into the  $(\text{CH}_3)_2\text{Cl}_2\text{Si}$  solution to decrease the surface energy. The contact angle of PDMS prepolymer on the silanized surface is smaller than that on the original surface, and the average depth of the microwells increases by about 50 nm at the same sphere interstice (shown in Table 1 and Figure 5). In fact, when the templates adsorb  $(\text{CH}_3)_2\text{Cl}_2\text{Si}$  molecules, not only does the surface energy decrease, but also the same network structure ( $-\text{OSi}(\text{CH}_3)_2-$ )<sub>n</sub> as PDMS prepolymer is formed on the surfaces. The surface energy is one of the important factors in wetting behavior. On the other hand, the same structure can also enhance the intermiscibility between PDMS prepolymer and the templates. To clarify what governs the wetting behavior of PDMS droplets in the present system, we have substituted a lower surface energy silane (OTS) for  $(\text{CH}_3)_2\text{Cl}_2\text{Si}$ . The results in Table 1 and Figure 5 confirm that the contact angle of PDMS prepolymer on the template modified by OTS molecules augments; however, the average depth of the microwells decreases at the same sphere interstice. Furthermore, the slope of the curve of the microwell depths versus the sphere interstices is smaller than the others when the templates are modified by OTS. These results clearly indicate that it is not the low-surface-energy molecules, but the same network structure that governs the wetting behavior of PDMS prepolymer.

In contrast, when we endowed hydrophilic hydroxyl ( $-\text{OH}$ ) groups on the silica spheres via plasma etching, the wettability of PDMS prepolymer on the hydrophilic surface weakened because of the different surface character. The contact angle of PDMS prepolymer on the hydrophilic surface is bigger than that on the template without decoration at the same sphere interstice, as shown in Table 1. Therefore, the depth of the microwells decreases by at least 30 nm, as presented in Figure 5. Moreover, it is noteworthy that, after plasma bombardment, not only were the silica spheres endowed with ( $-\text{Si}-\text{OH}$ ) groups, but also the surface roughness was induced due to plasma microscopically inhomogeneous etching as described previously.<sup>30</sup> To avoid such roughness on the template surfaces, the etching process was followed by an annealing treatment, but the surface roughness was still obvious on the PDMS molds as shown in Figure 4E,F. This is mainly attributable to adhesion force between PDMS and ( $-\text{Si}-\text{OH}$ ) groups. When the low-surface-energy PDMS prepolymer was cast on the silica spheres with high-surface-energy ( $-\text{Si}-\text{OH}$ ), the energy of the system was reduced dramatically due to the distinct surface energy, which leads to enhancement of the adhesion force between PDMS and silica spheres and makes PDMS molds break during the peeling process.

**Fabrication of Tetragonal ncp PDMS Molds.** By changing the arrangement of colloidal spheres, we can change the lattice structure of the microwells. In the experiment we prepared a template with tetragonal sphere arrays via mechanical stretching of the sphere-coated PDMS elastomers and transferred the spheres onto the PVA-coated substrate as reported previously.<sup>22</sup> After PDMS prepolymer was cast onto it and curing, a PDMS mold with tetragonal arrays of microwells can also be fabricated as shown in Figure 6. However, it is noteworthy that no saddle-sharp structure is present in the SEM and AFM images as hexagonal ncp arrays, due to the comparatively uniform interstices

(25) Nakajima, A.; Fujishima, A.; Hashimoto, K.; Watanabe, T. *Adv. Mater.* **1999**, *11*, 1365–1368.

(26) Feng, L.; Zhang, Z. Y.; Mai, Z. H.; Ma, Y. M.; Liu, B. Q.; Jiang, L.; Zhu, D. B. *Angew. Chem., Int. Ed.* **2004**, *43*, 2012–2014.

(27) Tsai, P. S.; Yang, Y. M.; Lee, Y. L. *Langmuir* **2006**, *22*, 5660–5665.

(28) Johnson, R. E., Jr.; Dettre, R. H. *Adv. Chem. Ser.* **1963**, *43*, 112–135.

(29) Nakae, H.; Inui, R.; Hirata, Y.; Saito, H. *Acta Mater.* **1998**, *46*, 2313–2318.

(30) Shiu, J. Y.; Kuo, C. W.; Chen, P. L.; Mou, C. Y. *Chem. Mater.* **2004**, *16*, 561–564.

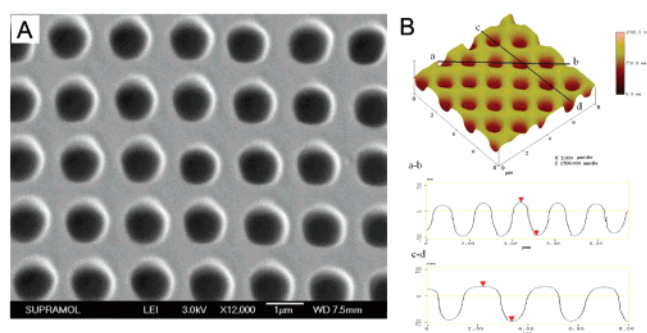


**Figure 6.** (A) SEM image of 2D tetragonal ncp microwells on the PDMS mold fabricated by using tetragonal ncp sphere arrays as the template. (B) AFM image and line profiles of tetragonal ncp microwells.

among spheres in the square lattice. The average depth of the microwells is more than 800 nm, almost equal to the size of the exposed silica sphere; moreover, the line profile along the corner direction exhibits a platform. This implies that PDMS prepolymer can penetrate the interstices absolutely under gravitation when the void among the spheres is big enough.

Besides PDMS, other polymers such as photopolymerized resin or thermosetting resin, can also be applied in making highly ordered ncp microwells on the surfaces using ncp colloidal crystals as templates, which can then be used as microlenses or microvials. Another great advantage of the approach is that PDMS molds can be easily peeled from the templates, which can be reused in making new molds.

### Conclusions

Highly ordered 2D ncp microwell arrays on a PDMS surface were prepared by replica molding using colloidal crystals as templates. The feature sizes of the microwells in width could be

flexibly controlled by the sphere interstices of the templates. The effects of the sphere interstices and chemical composition of the templates on the wetting behavior of PDMS prepolymer were studied. The wetting behavior of PDMS prepolymer on the rough surface is explained using Cassie–Baxter theory, because of the Wenzel roughness factor of the templates ( $>1.7$ ) and the high air ratio at the interface between the solid and prepolymer. The average sizes of the microwells in depth increase while the contact angles decrease with increasing sphere interstices. The prediction correlates well with experimental data. When the templates adsorb  $(\text{CH}_3)_2\text{Cl}_2\text{Si}$  molecules, the same network structure as PDMS prepolymer, formed on the surface, can enhance the intermiscibility between PDMS prepolymer and the templates, that is, the PDMS prepolymer contact angle. Consequently, the depths of the microwells increase. When hydrophilic hydroxyl ( $-\text{OH}$ ) groups are introduced onto the surfaces of the templates by plasma etching, surface roughness is induced on the PDMS molds. The distinct surface energy between PDMS prepolymer and templates leads to enhancement of the adhesion force and makes the PDMS molds break during the peeling process. The microwells on the PDMS surface here can find applications in cell patterning in the biology field or in microcontact printing as stamps. Filling the microwells with other materials may also lead to photonic or storage applications by reason of their small sizes.

**Acknowledgment.** This work was supported by the National Natural Science Foundation of China (Grant Nos. 20534040 and 90401020) and the program for Changjiang Scholars and Innovative Research Team in University (Grant No. IRT0422).

**Supporting Information Available:** Contact angles of water on the templates with decoration (Table S1). This material is available free of charge via the Internet at <http://pubs.acs.org>.

LA700333R